Acta Adriat., 25 (1/2): 139—159 (1984) YU ISSN: 0001—5113
AADRAY

SOME DYNAMIC PROPERTIES OF THE CHANNEL VIRSKO MORE (EASTERN ADRIATIC COAST)

NEKA DINAMIČKA SVOJSTVA VIRSKOG MORA

Mira Zore-Armanda and Vladimir Dadić

Institute of Oceanography and Fisheries, Split, Yugoslavia

Two large oceanographic experiments have been performed in the channel region Virsko more in 1975/76 and 1978/79. Current-meter data and some coastal phenomena like upwelling and response to wind forcing are described.

INTRODUCTION

In the frame of the investigations of possible location for the future nuclear power plant near Zadar complex oceanographic researches were carried out in the coastal region of the channel Virsko more (Vir Sea) from August 1975 to September 1976 and from September 1978 to March 1979 (Zore-Armanda, et al., 1977b; 1979a). During the first period characteristics of currents and other oceanographic parameters in the vicinity of Vir Island, as possible location for the power plant, were investigated. During the second period the whole region of Virsko more, which could be understood as the semiclosed basin, was studied. In this paper some dynamic characteristics of the region are described on the basis of the material collected in both periods.

MATERIAL AND METHODS

Alexeev current meters were used in the first experiment (Ferenčak, et al., 1977) and Aanderaa current meters in the second. Stations are given in Fig. 1. Measurement intervals are shown in Tables 1 and 2.

Table 1. Basic current measurement data — 1975/76

Station	Measurement depth (m)	Station depth (m)	Periods of observations	Measurement duration (hours)	Measurement intervals (minutes)	Number of data
1	3	58	15—17 8 75; 18—19 9 75; 11—13 12 75; 16—18 3 76; 13—15 4 76	206	5	2430
1	55	58	Same as for 3 m	135	5	1622
3	3	53	15 8—19 9 75; 11—15 12 75; 16 3—16 4 76; 15 6—14 9 76; 27 9— 1 10 76; 10 12—13 12 76	3996	5, 10 30, 60	14344
3	20	53	15 8—19 9 75; 11—16 12 75; 16 3—18 9 76; 27 9— 1 10 76; 10—13 12 76	4109	5, 10 30, 60	15868
3	45	53	Same as for 20 m	4120	5, 10 30, 60	15969
5	3	30	13—14 12 75; 17—18 3 76; 14—15 4 76; 13—18 8 76; 14—18 9 76	237	5	4118
5	25	30	13—14 12 75; 17—18 3 76; 14—15 4 76	66	5	793
6	3	12	13—14 12 75; 16—17 3 76; 13—14 4 76; 13—17 8 76; 14—18 9 76	246	5	2954
6	10	12	Same as for 3 m	238	5	2918
7	3	47	14—16 12 75; 18—19 3 76; 15—16 4 76	83	5	1005
7	45	47	Same as for 3 m	83	5	1005
8	3	23	14—16 12 75; 18—19 3 76; 15—16 4 76	81	5	975
8	15	23	Same as for 3 m	81	5	975
9	3	55	15—17 8 75; 18—20 9 75; 11—13 12 75; 16—18 3 76; 13—15 4 76; 16—18 6 76	274	5	3305
9	50	55	15—17 8 75; 18—20 9 75; 16—18 3 76; 13—15 4 76	169	5	1975
11	3	27	16—18 3 76	47	5	567
11	10	27	18—19 3 76	25	5	297
11	19	27	18—19 3 76	25	5	297
13	2	5	17—18 3 76	24	5	293
14	3	48	13—17 8 76; 14—18 9 76	193	5	2324
14	35	48	14—18 9 76	97	5	1171
15	3	45	13—17 8 76 14—18 9 76	193	5	2130
			Total	14748		77335

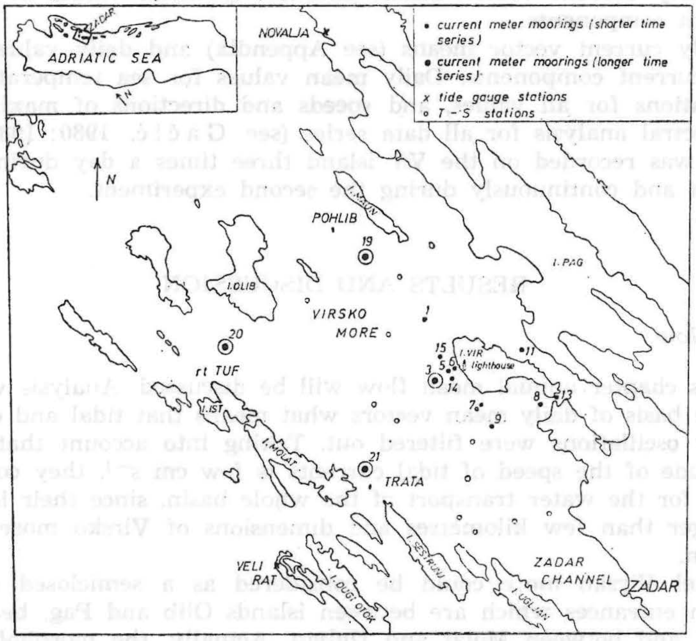

Fig. 1. Map of the study area

Table 2. Basic current measurement data — 1978/79

Station	Measu-rement depth (m)	Station depth (m)	Period of observations	Measu-rement duration (hours)	Measu-rement intervals (minutes)	Number of data
3	5	68	19—20 9 78	167	2	5030
(Vir)			28 2—23 3 79	545	10	3280
19	5	79	19—26 9 78	167	2	5022
(Pohlib)			28 2—18 3 79	438	10	2631
	56		19—26 9 78	167	2	5036
20	5	75	28 2—27 3 79	647	10	3884
(Tuf)	56		20—27 9 78	167	2	5031
			28 2—27 3 79	647	10	3886
21	5	57	19—26 9 78	167	2	5036
(Trata)			28 2—27 3 79	647	10	3886
	36	57	28 2—27 3 79	647	10	3883
Total				4407		41575

At most stations the sea temperature was also recorded. In addition, at a number of stations (Fig. 1) temperature and salinity data were collected on three occasions: 21—23 Sept. 1978, 24—25 Sept. 1978, 1—2 March 1979.

Statistical processing of current-meter data included:

a. Direction frequencies for eight principal directions and for every five-day interval (longer series) and the whole measurement interval. Speeds grouped in clasess of 5 cm s^{-1}.

b. Hourly current vector means and hourly mean values of north and east current components.

c. Daily current vector means (see Appendix) and daily values of north and east current components. Daily mean values for sea temperatures, standard deviations for all values, and speeds and directions of maximum flow.

d. Spectral analysis for all data series (see Gačić, 1980; 1983).

Wind was recorded on the Vir island three times a day during the first experiment and continuously during the second experiment.

RESULTS AND DISCUSSION

Residual flow

In this chapter annual mean flow will be discussed. Analysis was carried out on the basis of daily mean vectors what means that tidal and other high-frequency oscillations were filtered out. Taking into account that the order of magnitude of the speed of tidal currents is few cm s^{-1}, they could not be important for the water transport of the whole basin, since their lenght scale is not larger than few kilometres and dimensions of Virsko more are about 12×25 km.

Channel Virsko more could be considered as a semiclosed basin with three main entrances which are between islands Olib and Pag, between Olib and Molat and between Molat and Ugljan. Actually, the morphology of the basin is much more complex, but we consider that such simplification is sufficiently reliable for the development of the conception of the mean flow and water exchange with the outer sea.

Zadar channel, which extends southward from Virsko more, could be considered as the flowless corner. Namely, we have available the current-meter data for the location in the channel close to Zadar for four seasons 1975/76 (Zore-Armanda et al., 1977a) which show that essential characteristics of the flow in this channel are small residual speeds.

Table 3. Daily mean speeds (cm s^{-1}) and directions at location in front of Zadar (24-hour data series)

	Dec. 75	March 76	June 76	July 76	Aug. 76	Sept. 76
Surface layer	NW 3	N 2	N 2	0	0	S 1
Bottom layer	SE 3	NW 2	NW 2	SE 2	E 1	N 1

Compared with the speeds recorded in some other channels of the eastern Adriatic coast, these values are quite insignificant thus that they will be neglected hereinafter. Zadar channel extends to Pašman channel which ends with the shallow adjacent island Babac, which in turn makes barrier to the permanent incoming alongshore northwestern current, what may be the cause of small speeds.

To come to the representative annual values, all measurements performed in 1975/76 close to the Vir Island will be considered as if they belong to the same location. Stations to the north and east of the Vir Island (11 and 13) were not taken into consideration. Station 3, generalized in this way, is taken as representative of the vicinity of the Vir Island. It should be mentioned that deep measurements were performed at 45 m depth thus that they represent well the bottom layer since the station depth is 68 m.

Fig. 2 shows annual current roses for surface and bottom layer. The alongshore flow of the northwest direction is typical in the whole layer from surface to bottom. Following such general trend water enters the channel Virsko more through the sound Trata (between the islands Molat and Ugljan

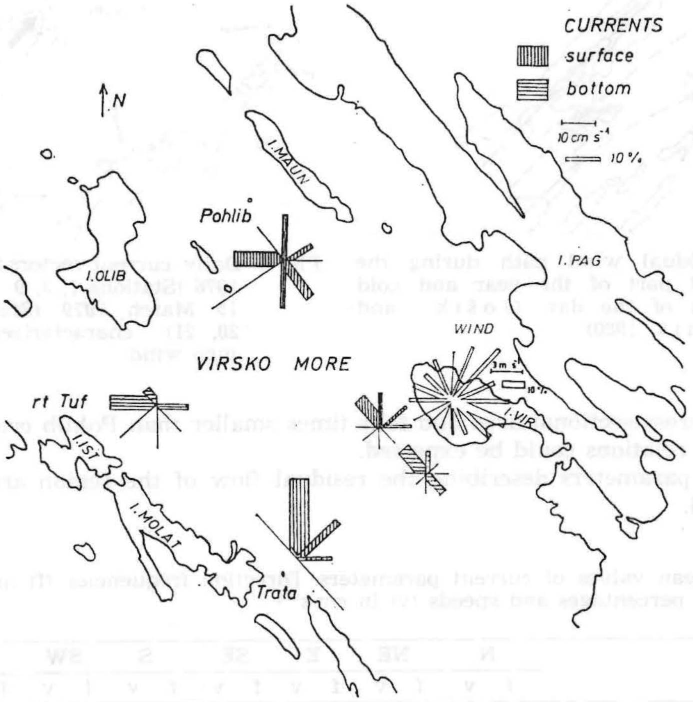

Fig. 2. Current roses for the whole year. Corresponding wind rose for the Vir island is constructed from two year data (July 1977 — June 1979)

— station 21) and leaves the basin through the sounds Pohlib (between islands Olib and Maun — station 19) and Tuf (between islands Olib and Ist — station 20). Alongshore northwest current is a part of the well known generally cyclonic circulation of the Adriatic Sea (see e.g. Zore-Armanda, 1968). In the region of Virsko more mean velocity of this flow is 11 cm s^{-1}. This mean flow represents the basic advection in all layers, what means that the channel Virsko more in the first approximation could be considered as a single layer basin. Generally, the air flow of the same direction prevails for the most part of the year (Fig. 3).

Fig. 2 shows also that the incoming current at the sound Trata is of higher velocity and frequency than the outgoing currents at sounds Pohlib and Tuf. As the cross-sectional area of the sound Trata is about three times smaller

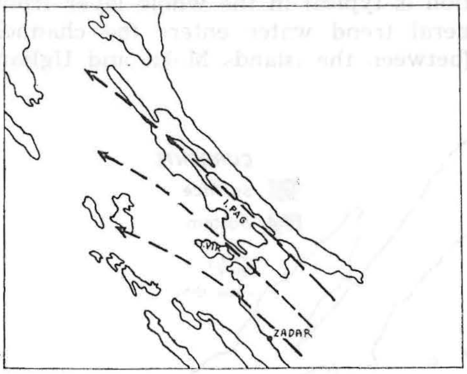

Fig. 3. Residual wind path during the cold part of the year and cold part of the day (Jošik and Šinik, 1980)

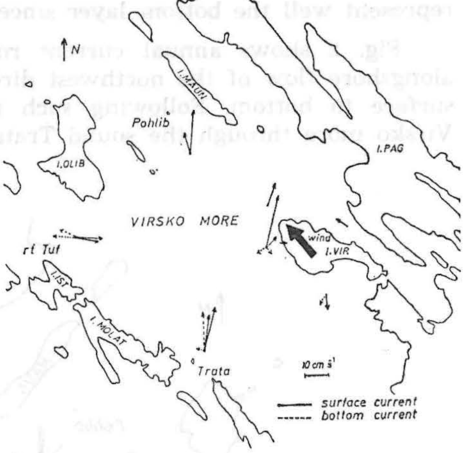

Fig. 4. Daily current vectors for 16 March 1976 (Stations 1, 3, 9, 11) and 14—15 March 1979 (Stations 3, 19, 20, 21) characterized by strong jugo wind

than Tuf cross-sectional area and four times smaller than Pohlib cross-sectional area, such relations could be expected.

Basic parameters describing the residual flow of the region are presented in Table 4.

Table 4. Mean values of current parameters. Direction frequencies (f) are expressed in percentages and speeds (v) in cm s^{-1}

		N		NE		E		SE		S		SW		W		NW	
		f	v	f	v	f	v	f	v	f	v	f	v	f	v	f	v
Vir	Surface	16	9	11	9	10	8	12	6	8	6	5	5	5	4	32	11
Pohlib	Surface	11	13	15	9	7	13	18	13	11	13	4	25	30	14	4	13
Trata	Surface	61	23	19	17	11	11	5	23							3	18
Vir	Bottom	10	6	4	5	7	4	21	7	7	5	4	4	7	5	43	10
Tuf	Bottom	2	1			14	10	2	9	2	7	6	15	47	14	25	6
All stations	Surface & Bottom	20	12	9	10	7	7	12	8	4	7	4	6	8	10	36	10

Table 4 shows clearly the prevalence of the northwest current. North direction is also frequent in the surface layer. It is most probably due to the most frequent jugo or scirocco wind (SE and ESE). In the same way the west current direction could be, at least partly, due to the bura or bora wind (NE — ENE), as it has been found elsewhere along the eastern Adriatic coast (Zore-Armanda et al., 1979). Thus currents influenced by local factors are superimposed on the basic northwest flow of the East Adriatic coastal region. It seems that fresh water impact and E-P factor could be neglected. Summer surface salinity (Figs. 7 and 10) decreases going off the coast showing poor influence of the Zrmanja River to salinity distribution and flow in the channel Virsko more. On the other hand, as it will be seen later on, wind influences horizontal and vertical circulation.

Seasonal variations and response to the wind forcing

In winter typical winds are from ESE to SE (jugo, scirocco) and from NNE to ENE (bura). Jugo is more frequent than bura in this region. Jugo is alongshore wind and it induces shoreward surface transport right of the wind direction (G a č i ć, 1980). Compensatory current of the offshore direction appears in the bottom layer. Fig. 4 shows the circulation in the surface and bottom layers for situation with jugo wind. Onshore current is superimposed on the northwest current in the surface layer. Thus water enters the basin at Tuf and Trata sounds in the surface layer. As shown by Fig. 4 the outgoing current appears in the bottom layer of the Trata sound. Thus vertical circulation is formed in the way that surface water enters the basin Virsko more and bottom water leaves itd.

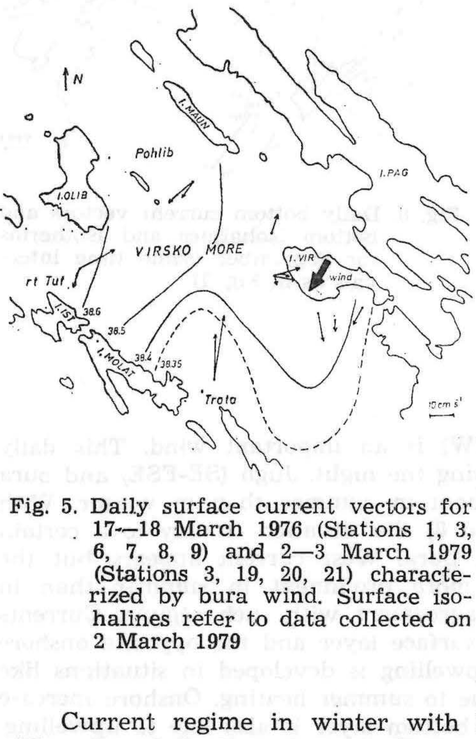

Fig. 5. Daily surface current vectors for 17—18 March 1976 (Stations 1, 3, 6, 7, 8, 9) and 2—3 March 1979 (Stations 3, 19, 20, 21) characterized by bura wind. Surface isohalines refer to data collected on 2 March 1979

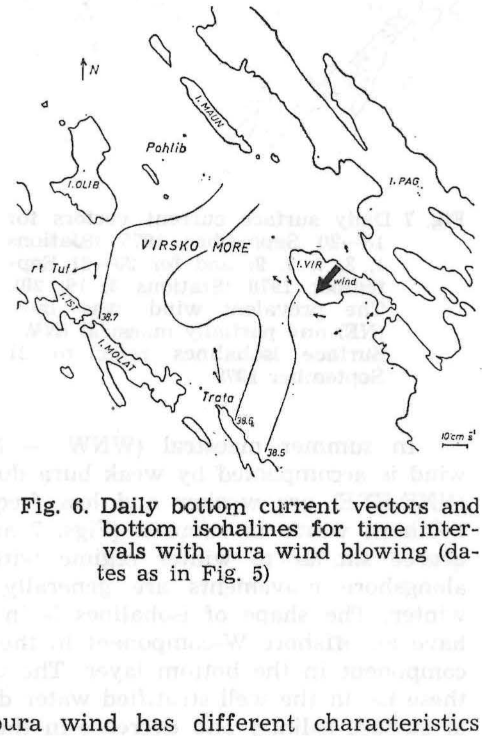

Fig. 6. Daily bottom current vectors and bottom isohalines for time intervals with bura wind blowing (dates as in Fig. 5)

Current regime in winter with bura wind has different characteristics (Figs. 5 and 6). Bura is typically catabatic wind due to the presence of the mountains along the coast. It brings cold and dry air and its local direction (NNE to ENE) depends on the orogenic properties of the coast. Thus, rather strong horizontal wind shear may appear along the coast. Most probably due to this phenomenon bura induces two gyres in the surface layer: cyclonic northward one to the line Trata-Vir and anticyclonic one south from that line. In this way in the middle of the basin and in the vicinity of the Vir island the induced current has the opposite direction of bura. Surface isohalines also follow such pattern. It seems that the vertical shear does not appear and upwelling, which otherwise clearly appears with bura in the warm part of the year, could not be noticed. The current field is vertically more homogeneous with bura than with jugo which induces clear vertical circulation.

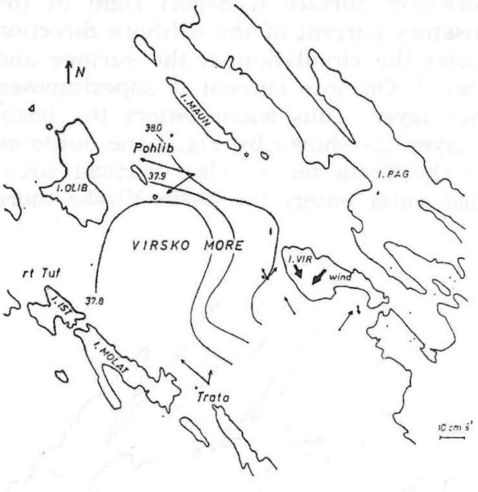

Fig. 7 Daily surface current vectors for 18—20 September 1975 (Stations 1, 3, 7, 7, 9) and for 20—21 September 1978 (Stations 3, 19, 20). The prevalent wind was bura (NE) and partially maestral (NW). Surface isohalines refer to 21 September 1978

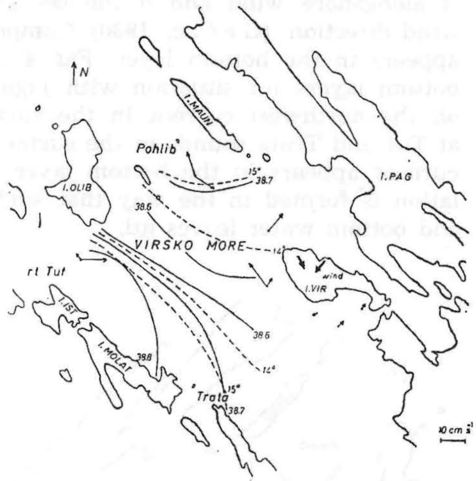

Fig. 8. Daily bottom current vectors and bottom isohalines and isotherms for September (same time intervals as in Fig. 7)

In summer maestral (WNW — NW) is an important wind. This daily wind is accompanied by weak bura during the night. Jugo (SE-ESE) and bura (NNE-ENE) are weaker and less frequent in summer than in winter. With northern winds in summer (Figs. 7 and 8) the situation is only to a certain degree similar to winter regime with bura. West current appears but the alongshore movements are generally more prominent in summer than in winter. The shape of isohalines is in agreement with such regime. Currents have an offshore W-component in the surface layer and the opposite onshore component in the bottom layer. The upwelling is developed in situations like these i.e. in the well stratified water due to summer heating. Onshore increase of surface salinity and decrease in the bottom layer is also due to upwelling. Fig. 9 clearly shows the appearance of upwelling on 2—23 September 1978. Prevalence of bura (NE wind) is shown by negative W and S wind components on 20 and 21 September. The air temperature decreased at the same time in agreement with regular appearance of cold and dry air which penetrated with bura to the coastal region. On the next day after the start of bura wind, the sea temperature decreased and continued to decrease two

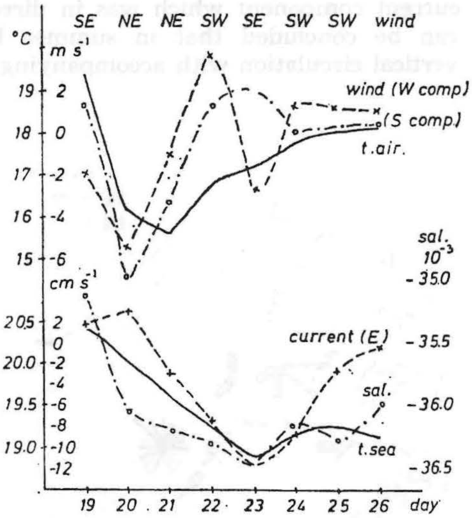

Fig. 9. Daily means of meteorological and oceanographic parameters for September 1978 which correspond to time interval in Figs. 7 and 8. Meteorological parameters are observed at the lighthouse of Vir island and oceanographic parameters at Station 3.

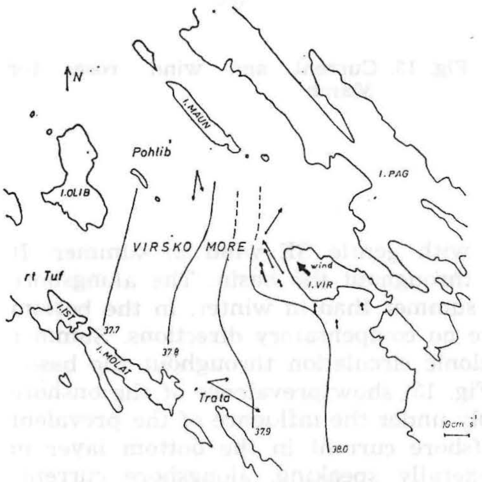

Fig. 10. Daily surface current vectors for 15—16 August 1975 (Stations 1, 7, 8, 9), 17 September 1976 (Stations 6, 14, 15) and 22—23 September 1978 (Stations 3, 19, 21) always with poor SE wind (jugo). Surface isohalines refer to 22—23 September 1978

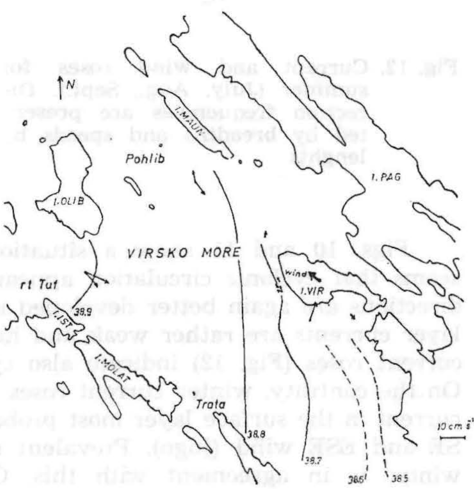

Fig. 11. Daily bottom current vectors and bottom isohalines for the same time intervals as in Fig. 10

days after bura stopped. Salinity increase at the same time showed the process of upwelling since it brought saltier water from deeper layers to the surface. Temperature decrease and salinity increase appeared with decrease of east current component which was in direct connection with bura forcing. Thus it can be concluded that in summer bura and other northern winds induce vertical circulation with accompanying uppwelling.

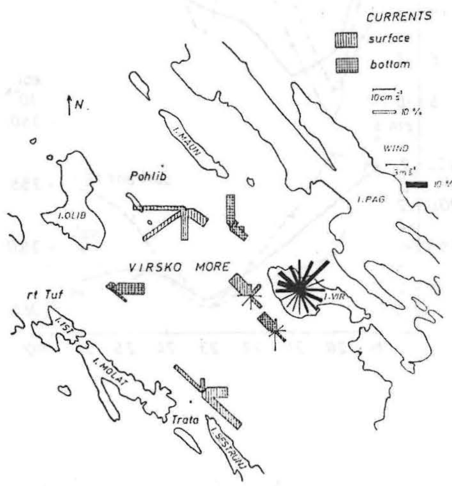

Fig. 12. Current and wind roses for summer (July, Aug., Sept.). Direction frequencies are presented by breadths and speeds by lenghts

Fig. 13. Current and wind roses for March

Figs. 10 and 11 show a situation with gentle SE wind in summer. It seems that cyclonic circulation appears throughout the basin. The alongshore directions are again better developed in summer than in winter. In the bottom layer currents are rather weak and have no compensatory directions. Summer current roses (Fig. 12) indicate also cyclonic circulation throughout the basin. On the contraty, winter current roses (Fig. 13) show prevalence of the onshore current in the surface layer most probably under the influence of the prevalent SE and ESE wind (jugo). Prevalent offshore current in the bottom layer in winter is in agreement with this. Generally speaking, alongshore currents are mostly normal to the coast.

Vertical stratification of properties and consequently the density (Fig. 14) are other essential differences between summer and winter. This may result in different response of the sea to the wind forcing (Gačić, 1980). Current regime in spring and autumn could prove such statement. Spring (April, May, June) has similarity to both summer and winter since both north and north-west currents are developed in the middle of the basin (Fig. 15). We can see also that stratification begins in April and develops well until June. Thus June situation with jugo is very similar to summer situation with jugo (Figs. 16 c, 10 and 11). April situation with northern winds is similar to winter situation with bura (Figs. 16 b and 5). However, due to the beginning of

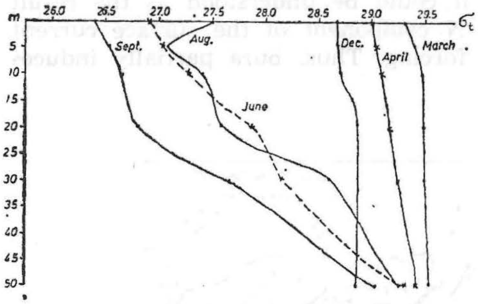

Fig. 14. Vertical distribution of density at Station 3 in different months

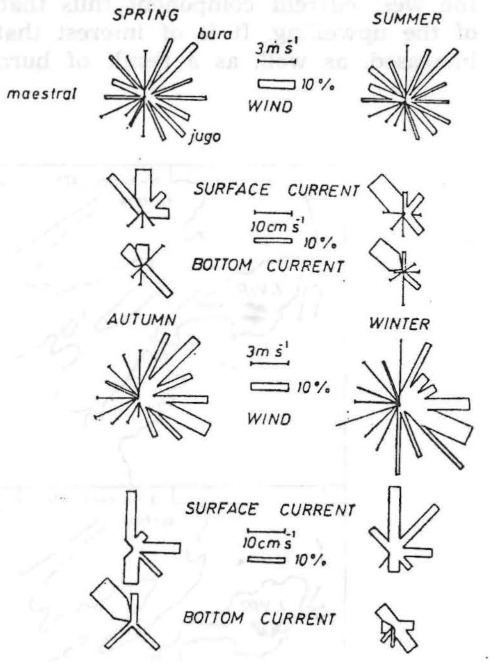

Fig. 15. Seasonal wind roses for island Vir and corresponding surface and bottom current roses for Station 3 in the vicinity of island Vir

surface heating in April some stratification has already been present in that month and bura wind is accompanied with upwelling (see Table 5).

Table 5. Meteorological and oceanographic parameters from April 1976 showing decreased sea surface temperature caused by upwelling due to bura wind forcing. Data refer to Station 3 and lighthouse at Vir island

Date	Wind at Vir lighthouse (speed in m s^{-1}) 7 a.m.	2 p.m.	9 p.m.	Daily mean temperature (°C) Vir lighthouse air	sea surface	Sea water temperature (°C) at 2 p.m. Station 3 surface	bottom	Surface current at Station 3 (cm s^{-1}) daily mean E comp.	N comp.
5	$SE_{3.0}$	C	C	13.2	13.3	13.0	10.5	7.9	—2.2
6	C	$W_{0.5}$	C	12.5	13.4	13.0	10.0	6.9	—1.0
7	$E_{0.5}$	$SE_{2.0}$	C	12.7	13.5	13.2	10.2	5.2	6.9
8	$NNE_{3.5}$	$NE_{6.0}$	$NE_{6.5}$	9.9	13.0	13.0	11.0	—5.6	4.7
9	$NNE_{18.0}$	$NNE_{12.0}$	$NNE_{14.5}$	9.5	10.4	—	—	—18.8	15.2
10	$NNE_{10.5}$	$NE_{8.5}$	$NE_{7.0}$	9.5	10.5	—	—	1.3	17.4
11	$NE_{6.0}$	$NE_{6.5}$	$NE_{4.0}$	11.3	11.0	—	—	10.1	2.4
12	$SE_{0.6}$	$NE_{6.0}$	$NE_{1.5}$	13.8	11.4	11.4	10.5	—	—

On 8 and 9 April W current component developed after the start of bura blowing. It reached high speed (18.8 cm s^{-1}) the same day bura reached violent speed (18 m s^{-1}). Both NE and NNE are bura directions. Air temperature changed as soon as bura started. Bura always carries cold air as it blows from the mountains and brings continental air to the coastal zone. Sea surface temperature strongly decreased the second day after the development of the west current component thus that it could be understood as the result of the upwelling. It is of interest that N component of the surface current increased, as well, as a result of bura forcing. Thus, bura partially induces

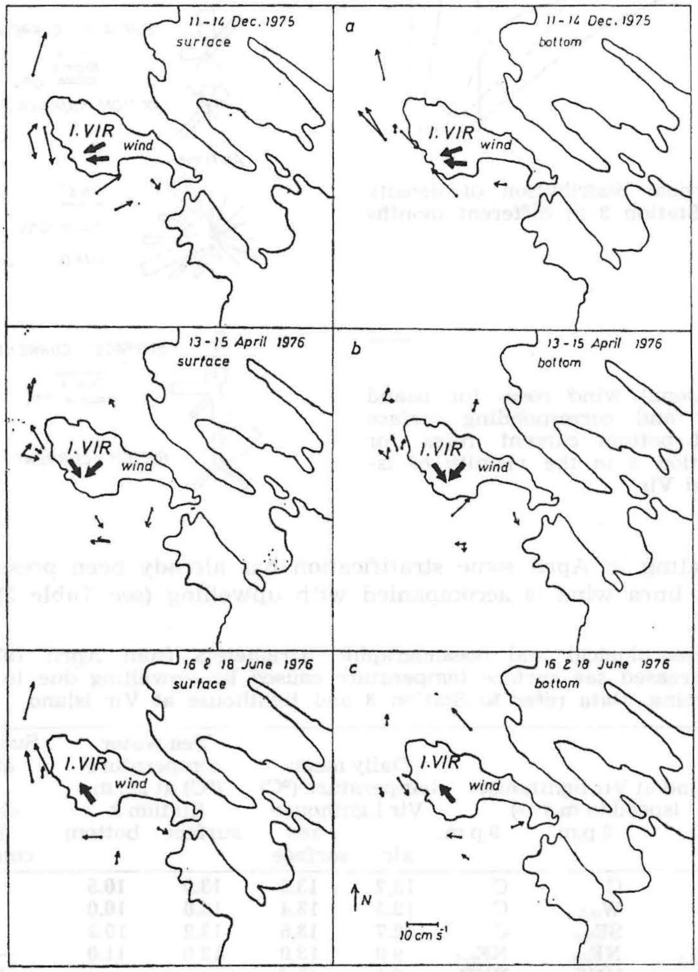

Fig. 16. Daily current vectors for different wind situations in autumn and spring in the vicinity of Vir island

the current of the opposite direction at this location. We have seen that the same happened in winter at this location (Fig. 5), since bura induced horizontal gyres in the whole basin.

Autumn circulation is similar to winter circulation (Figs. 15 and 16a). The only difference between them is the development of the NW current in the bottom layer in autumn what is similar to summer regime.

CONCLUSIONS

Channel Virsko more in the first approximation could be considered as a single layer basin with generally alongshore northwest current of mean velocity of 11 cm s^{-1}.

Zadar channel could be considered as a flowless corner of the basin. Generally speaking water enters the basin through the sound Trata and leaves it through the sounds Pohlib and Tuf.

Currents induced by wind forcing are superimposed on this basic northwest flow of the east Adriatic coastal region. The response to wind forcing is different in different seasons probably due to variations in density stratification.

In winter, alongshore jugo wind (SE to ESE) induces onshore current in the surface layer with compensatory offshore current in the bottom layer. In summer, it induces cyclonic circulation in the surface layer without compensatory movements in the bottom layer.

Bura, i.e. wind normal to the coast (NNE to ENE) induces two gyres in winter: cyclonic north from the line Trata-Vir and anticyclonic south of that line. Vertical shear could not be noticed. It is assumed that such pattern is due to rather strong horizontal wind shear along the coast which is typical for bura. In summer, bura and other northern winds induce currents with offshore W-component in the surface layer and the opposite onshore component in the bottom layer. Accompanying upwelling is evident from temperature and salinity data.

Thus, under stratified conditions (summer) alongshore jugo wind induces horizontal circulation without bottom compensatory movements and in the nonstratified situation well developed vertical circulation. On the contrary, northern bura wind under stratified conditions induces vertical circulation (offshore in the surface layer with upwelling) and horizontal gyres in the nonstratified situation.

REFERENCES

Ferenčak, M., I. Nožina i Z. Vučak, 1977. Metodika mjerenja struje i pokus s plovcima. Nuklearna elektrana Vir kod Zadra, Oceanografska, biološka i meteorološka istraživanja Virskog akvatorija, Studije i elaborati (Technical reports), Institut za oceanografiju i ribarstvo, Split, 22 (1) : 24—25.

Gačić, M. 1980. Some characteristics of the response of the Adriatic Sea coastal region to the atmospheric forcing. Acta Adriat., 21 (2) : 239—254.

Gačić, M. 1983. Dugoperiodičke oscilacije u strujnom polju u Jadranu. Doktorska disertacija, Beograd,

Jošić, D. i N. Šinik. 1980. Prosječni difuzni potencijal okoliša NE Vir, Studije, Republički hidrometeorološki zavod SR Hrvatske, Centar za meteorološka istraživanja, Zagreb,

Zore-Armanda, M. 1968. The system of currents in the Adriatic Sea. Stud. Rev. gen. Fish. Coun. Medit., 34 : 1—48.

Zore-Armanda, M. and collaborators, 1977a. Oceanografsko-biološka svojstva mora u Zadarskom kanalu, Studije i elaborati (Technical reports), Institut za oceanografiju i ribarstvo, Split,

Zore-Armanda, M. and collaborators, 1977b. Nuklearna elektrana Vir kod Zadra, Oceanografska, biološka i meteorološka istraživanja Virskog akvatorija, Studije i elaborati, (Technical reports), Institut za oceanografiju i ribarstvo, Split, 22 (1—4).

Zore-Armanda, M., M. Bone, M. Gačić, Z. Janjić, V. Dadić i A. Puškarić, 1979a. Nuklearna elektrana Vir kod Zadra, Oceanografsko-biološka istraživanja, Studije i elaborati (Technical reports), Institut za oceanografiju i ribarstvo, Split, 39 (1/2).

Zore-Armanda, M., M. Bone i M. Gačić, 1979b. Some dynamic characteristic of the East Adriatic coastal area. Acta Adriat., 9 (10): 83—102.

NEKA DINAMIČKA SVOJSTVA VIRSKOG MORA

Mira Zore-Armanda i Vladimir Dadić

Institut za oceanografiju i ribarstvo, Split, Jugoslavija

KRATKI SADRŽAJ

U okviru istraživanja Virskog mora kao moguće lokacije za izgradnju nuklearne elektrane, izvedena su dva oceanografska eksperimenta u toku 1975/76. i 1978/79. godine. U ovom radu su iskorišteni strujomjerni podaci tih eksperimenata za određivanje karakteristika rezidualnog strujanja. Istražene su sezonske promjene, utjecaj vjetra i fenomen upwellinga.

Virsko more se u prvoj aproksimaciji može shvatiti kao jednoslojni bazen s dužobalnim sjeverozapadnim smjerom strujanja prosječne brzine od 11 cm s^{-1}. S aspekta strujanja Zadarski se kanal može shvatiti kao mrtvi džep. Uopćeno voda u Virsko more ulazi kroz prolaz Trata a izlazi kroz prolaze Pohlib i Tuf.

Na osnovno sjevernozapadno strujanje superponira se strujanje prouzročeno vjetrom. Odgovor mora na djelovanje vjetra se mijenja prema sezoni, vjerojatno zbog različite stratifikacije.

Zimski dužobalni vjetar — jugo potakne u površinskom sloju strujanje prema obali s kompenzacijskim strujanjem prema otvorenom moru u pridnenom sloju. Ljeti jugo potakne u površinskom sloju ciklonalnu cirkulaciju bez kompenzacijskog strujanja u pridnenom sloju.

Bura puše okomito na obalu i zimi uvjetuje dva vrtloga: ciklonalni sjeverno od linije Trata-Vir i anticiklonalni južno od te linije. Nije uočeno vertikalno smicanje. Pretpostavljeno je da je takav tip strujanja uvjetovan horizontalnim smicanjem u polju vjetra, što je tipično za buru. Ljeti bura i drugi sjeverni vjetrovi potaknu u površinskom sloju strujanje od obale s naglašenom zapadnom komponentom. Kompenzacijsko strujanje u pridnenom sloju ima smjer prema obali a praćeno je pojavom upwellinga koja se može uočiti na podacima o temperaturi i salinitetu.

Prema tome, uz razvijenu stratifikaciju (ljeti) jugo potiče horizontalnu cirkulaciju bez kompenzacijskog strujanja u pridnenom sloju a u nestratificiranom moru (zimi) razvijenu vertikalnu cirkulaciju. Obrnuto, bura uz razvijenu stratifikaciju potiče vertikalnu cirkulaciju s upwellingom a horizontalno razvijene vrtloge u nestratificiranom moru.

APPENDIX
Daily current vectors

Station	Date	Surface Azimuth°	Surface Speed cm s−1	Bottom Azimuth°	Bottom Speed cm s−1
1	15 8 75	38	13	1	3
3	16 8 75	318	15	137	11
3	17 8 75	327	11	137	3
3	18 8 75	324	5	327	10
3	19 8 75	46	6	325	10
3	20 8 75	352	10	327	15
3	21 8 75	342	5	324	11
3	22 8 75	333	9	325	5
3	23 8 75	325	14	133	7
3	24 8 75	330	24	118	9
3	25 8 75	313	17	147	2
3	26 8 75	326	6	332	17
3	27 8 75	328	21	331	33
3	28 8 75	353	17	327	28
3	29 8 75	44	10	325	9
3	30 8 75	125	10	148	11
3	31 8 75	155	9	145	5
3	1 9 75	135	13	103	1
3	2 9 75	142	7	130	5
3	3 9 75	87	5	144	9
3	4 9 75	66	1	126	3
3	5 9 75	139	2	325	10
3	6 9 75	149	3	327	12
3	7 9 75	338	6	332	7
3	8 9 75	328	9	352	3
3	9 9 75	350	6	322	14
3	10 9 75	301	8	323	14
3	11 9 75	23	5	157	4
3	12 9 75	171	5	145	12
3	13 9 75	163	10	331	4
3	14 9 75	110	5	316	14
3	15 9 75	313	16	113	13
3	16 9 75	320	7	158	6
3	17 9 75	345	5	329	21
3	18 9 75	331	8	326	22
5	16 8 75	318	5	140	1
6	16 8 75	331	6	360	0
7	15 8 75	359	5	7	14
8	16 8 75	332	1	—	—
9	15 8 75	353	2	132	1
1	18 9 75	13	6	45	11
7	20 9 75	331	12	249	1
8	20 9 75	180	3	55	1
9	18 9 75	41	12	50	2
1	11 12 75	13	15	342	11
3	11 12 75	39	4	323	17
3	12 12 75	41	3	321	14
3	13 12 75	159	6	324	9
3	14 12 75	163	8	332	13
5	13 12 75	164	12	356	3
6	13 12 75	155	15	135	9
7	14 12 75	63	4	325	14
8	14 12 75	139	5	275	4
9	11 12 75	73	6	—	4
1	16 3 76	19	11	—	—

Station	Date	Surface Azimuth°	Surface Speed cm s^{-1}	Bottom Azimuth°	Bottom Speed cm s^{-1}
1	17 3 76	22	11	—	—
3	16 3 76	140	4	244	4
3	17 3 76	133	4	332	2
3	18 3 76	146	5	77	6
3	19 3 76	158	4	125	5
3	20 3 76	171	6	129	6
3	21 3 76	136	5	183	3
3	22 3 76	120	5	179	6
3	23 3 76	152	4	271	5
3	24 3 76	201	6	128	7
3	25 3 76	253	4	—	—
3	27 3 76	54	5	309	2
3	28 3 76	247	3	148	10
3	29 3 76	86	8	285	7
3	30 3 76	113	5	334	9
3	31 3 76	77	9	317	10
5	17 3 76	110	6	150	5
6	16 3 76	87	3	98	2
7	18 3 76	169	12	278	4
8	18 3 76	213	9	74	3
9	16 3 76	164	6	220	3
9	17 3 76	213	5	250	2
1	14 4 76	28	7	339	6
1	15 4 76	1	6	95	4
3	1 4 76	69	7	326	4
3	2 4 76	60	8	330	3
3	3 4 76	76	8	291	6
3	4 4 76	82	6	343	1
3	5 4 76	105	8	331	2
3	6 4 76	99	7	266	2
3	7 4 76	37	9	162	2
3	8 4 76	310	7	115	19
3	9 4 76	308	24	134	7
3	10 4 76	4	17	311	15
3	11 4 76	77	10	322	8
3	12 4 76			318	7
3	13 4 76	105	6	314	8
3	14 4 76	86	4	329	4
5	14 4 76	131	1	333	7
6	13 4 76	329	8	3	2
7	15 4 76	160	5	40	9
8	15 4 76	205	7	160	4
9	14 4 76	268	3	149	1
9	15 4 76	257	5	247	1
11	14 4 76	304	2	359	3
11	15 4 76	340	2	28	2
13	13 4 76	250	1	—	—
1	17 4 76	11	22	79	3
1	18 6 76	19	13	332	7
3	15 6 76	21	4	307	4
3	16 6 76	332	22	130	12
3	17 6 76	352	12	228	3
3	19 6 76	129	3	323	13
3	20 6 76	346	7	318	4
3	21 6 76	347	7	152	5
3	22 6 76	78	6	145	12
3	23 6 76	180	3	131	7

Station	Date	Surface Azimuth°	Surface Speed cm s^{-1}	Bottom Azimuth°	Bottom Speed cm s^{-1}
3	24 6 76	1	5	170	10
3	25 6 76	320	10	277	5
3	26 6 76	342	15	314	12
3	27 6 76	353	7	332	12
3	28 6 76	351	11	340	12
3	29 6 76	58	7	321	4
3	30 6 76	49	4	319	6
5	15 6 76	4	5	147	7
6	15 6 76	330	11	99	1
7	15 6 76	285	5	283	5
8	15 6 76	119	5	70	3
9	17 6 76	303	1	160	2
9	18 6 76	350	3	320	3
11	17 6 76	263	2	327	7
11	18 6 76	128	1	303	13
3	1 7 76	352	6	296	3
3	2 7 76	32	7	145	4
3	3 7 76	102	4	2	1
3	4 7 76	126	6	141	2
3	5 7 76	57	2	152	6
3	7 7 76	228	1	148	9
3	8 7 76	122	2	290	1
3	9 7 76	146	11	347	7
3	10 7 76	146	7	335	6
3	11 7 76	164	3	126	5
3	12 7 76	154	6	43	6
3	13 7 76	161	4	23	1
3	14 7 76	159	14	309	7
3	15 7 76	163	13	323	9
3	16 7 76	156	11	352	7
3	17 7 76	150	5	322	6
3	18 7 76	248	3	144	5
3	19 7 76	9	5	116	3
3	20 7 76	147	2	327	3
3	21 7 76	333	5	316	9
3	22 7 76	321	8	337	7
3	23 7 76	117	5	117	1
3	24 7 76	100	4	320	23
3	25 7 76	238	1	321	26
3	26 7 76	261	5	242	1
3	27 7 76	252	5	330	11
3	28 7 76	192	1	307	1
3	29 7 76	—	5	122	6
3	30 7 76	347	4	172	4
3	31 7 76	38	2	197	6
3	1 8 76	325	8	125	10
3	2 8 76	327	16	325	14
3	3 8 76	27	11	327	19
3	4 8 76	92	7	323	21
3	5 8 76	330	14	344	8
3	6 8 76	328	18	131	6
3	7 8 76	303	9	75	3
3	8 8 76	289	4	333	12
3	9 8 76	93	2	290	2
3	10 8 76	50	3	150	8
3	11 8 76	111	10	327	5
3	12 8 76	155	12	322	15
3	13 8 76	176	5	327	12

Station	Date	Surface Azimuth°	Surface Speed cm s−1	Bottom Azimuth°	Bottom Speed cm s−1
3	14 8 76	326	6	63	3
3	15 8 76	—	—	125	7
3	16 8 76	—	—	146	13
3	18 8 76	12	8	332	11
3	19 8 76	337	15	327	19
3	20 8 76	325	16	322	18
3	21 8 76	305	7	320	19
3	22 8 76	324	10	76	3
3	23 8 76	331	15	134	9
3	24 8 76	319	14	317	6
3	25 8 76	296	7	333	8
3	26 8 76	296	8	324	4
3	27 8 76	309	5	242	2
3	28 8 76	337	4	155	2
3	29 8 76	271	3	158	8
3	30 8 76	112	2	341	5
5	13 8 76	323	6	57	2
5	14 8 76	350	9	—	—
5	15 8 76	321	9	—	—
5	16 8 76	327	18	—	—
6	13 8 76	324	3	336	1
6	14 8 76	313	3	97	1
6	15 8 76	323	3	326	5
6	16 8 76	322	6	298	2
14	14 8 76	306	3	331	5
14	15 8 76	313	2	327	3
14	16 8 76	333	4	351	2
14	17 8 76	311	7	87	2
15	13 8 76	284	3	315	3
15	14 8 76	321	3	311	3
15	15 8 76	310	4	331	1
15	16 8 76	324	8	305	3
3	31 8 76	33	7	331	7
3	1 9 76	11	8	303	2
3	2 9 76	322	2	77	1
3	3 9 76	23	8	86	10
3	4 9 76	324	18	159	21
3	5 9 76	118	19	310	13
3	6 9 76	328	1	336	26
3	7 9 76	18	9	315	4
3	8 9 76	272	7	232	7
3	9 9 76	309	6	92	2
3	10 9 76	341	8	83	9
3	11 9 76	330	17	137	16
3	12 9 76	311	6	22	3
3	13 9 76	59	12	330	23
3	18 9 76	321	19	347	5
3	19 9 78	269	1	—	—
3	20 9 78	37	6	—	—
3	21 9 78	301	3	—	—
3	22 9 78	308	9	—	—
3	23 9 78	304	16	—	—
3	24 9 78	292	10	—	—
3	25 9 78	243	2	—	—
3	26 9 78	172	2	—	—
3	27 9 76	52	12	318	3
3	28 9 76	320	13	162	7
3	29 9 76	262	22	156	11

Station	Date	Surface Azimuth°	Surface Speed cm s^{-1}	Bottom Azimuth°	Bottom Speed cm s^{-1}
3	30 9 76	334	6	358	4
5	14 9 76	314	5	—	—
5	15 9 76	321	15	—	—
5	16 9 76	331	21	32	14
5	19 9 76				
6	15 9 76	321	9	342	8
6	16 9 76	325	16	318	13
6	17 9 76	341	18	351	12
6	18 9 76	329	12	—	—
14	15 9 76	313	3	315	13
14	16 9 76	333	4	314	17
14	17 9 76	341	4	323	10
14	18 9 76	320	5	317	11
15	15 9 76	326	3	—	—
15	16 9 76	347	7	—	—
15	17 9 76	344	9	—	—
15	18 9 76	332	7	—	—
3	10 12 76	17	12	356	10
3	11 12 76	78	22	330	15
3	12 12 76	250	3	332	11
19	19 9 78	158	6	28	2
19	20 9 78	291	24	125	10
19	21 9 78	229	25	350	21
19	22 9 78	175	20	350	9
19	23 9 78	155	17	151	11
19	24 9 78	163	9	106	5
19	25 9 78	155	11	139	4
19	26 9 78	153	12	300	1
20	20 9 78	—	—	319	4
20	21 9 78	—	—	110	21
20	22 9 78	—	—	110	13
20	23 9 78	—	—	130	9
20	24 9 78	—	—	101	8
20	25 9 78	—	—	4	1
20	26 9 78	—	—	332	1
20	27 9 78	—	—	306	1
21	20 9 78	16	6	—	—
21	21 9 78	322	18	—	—
21	22 9 78	68	11	—	—
21	23 9 78	119	27	—	—
21	24 9 78	122	19	—	—
21	25 9 78	94	10	—	—
21	26 9 78	112	14	—	—
21	27 9 78	112	10	—	—
3	28 2 79	24	26	—	—
3	1 3 79	28	30	—	—
3	2 3 79	72	14	—	—
3	3 3 79	97	11	—	—
3	4 3 79	88	7	—	—
3	5 3 79	166	7	—	—
3	6 3 79	200	4	—	—
3	7 3 79	21	8	—	—
3	8 3 79	358	20	—	—
3	9 3 79	26	14	—	—
3	10 3 79	9	27	—	—
3	11 3 79	26	13	—	—
3	12 3 79	43	16	—	—
3	13 3 79	83	9	—	—
3	14 3 79	69	17	—	—

Station	Date	Surface Azimuth°	Surface Speed cm s⁻¹	Bottom Azimuth°	Bottom Speed cm s⁻¹
3	15 3 79	21	24	—	—
3	16 3 79	93	8	—	—
3	17 3 79	141	10	—	—
3	18 3 79	355	12	—	—
3	19 3 79	326	12	—	—
3	20 3 79	23	13	—	—
3	21 3 79	53	10	—	—
3	22 3 79	49	15	—	—
3	23 3 79	280	10	—	—
19	28 2 79	293	13	—	—
19	1 3 79	253	16	—	—
19	2 3 79	216	15	—	—
19	3 3 79	213	9	—	—
19	4 3 79	171	10	—	—
19	5 3 79	206	10	—	—
19	6 3 79	41	14	—	—
19	7 3 79	22	12	—	—
19	8 3 79	312	16	—	—
19	9 3 79	250	9	—	—
19	10 3 79	269	8	—	—
19	11 3 79	59	4	—	—
19	12 3 79	53	10	—	—
19	13 3 79	30	9	—	—
19	14 3 79	357	9	—	—
19	15 3 79	12	19	—	—
19	16 3 79	85	10	—	—
19	17 3 79	136	18	—	—
19	18 3 79	102	16	—	—
20	1 3 79	104	25	97	4
20	2 3 79	59	19	182	7
20	3 3 79	200	7	255	13
20	4 3 79	131	13	233	6
20	5 3 79	109	17	316	10
20	6 3 79	113	21	311	12
20	7 3 79	99	23	336	2
20	8 3 79	102	21	69	2
20	9 3 79	84	19	322	13
20	10 3 79	101	21	294	6
20	11 3 79	101	30	289	11
20	12 3 79	103	20	302	6
20	13 3 79	85	21	273	10
20	14 3 79	93	11	285	10
20	15 3 79	99	10	278	12
20	16 3 79	310	27	222	24
20	17 3 79	302	40	258	28
20	18 3 79	295	23	292	23
20	19 3 79	294	9	266	17
20	20 3 79	218	6	287	9
20	21 3 79	123	8	271	16
20	23 3 79	74	16	260	14
20	24 3 79	91	17	291	9
20	25 3 79	98	20	288	11
20	26 3 79	114	15	284	7
20	27 3 79	57	10	242	13
20	28 3 79	306	21	265	17
21	1 3 79	14	25	7	20
21	2 3 79	13	29	334	6
21	3 3 79	5	20	348	15
21	4 3 79	345	11	250	33

Station	Date	Surface Azimuth°	Surface Speed cm s^{-1}	Bottom Azimuth°	Bottom Speed cm s^{-1}
21	5 3 79	12	12	294	22
21	6 3 79	36	17	284	19
21	7 3 79	66	17	287	15
21	8 3 79	51	12	283	18
21	9 3 79	45	23	297	15
21	10 3 79	30	14	264	15
21	11 3 79	25	23	281	5
21	12 3 79	20	21	141	1
21	13 3 79	9	24	140	2
21	14 3 79	9	15	303	2
21	15 3 79	8	20	12	18
21	16 3 79	353	38	317	13
21	17 3 79	342	35	257	30
21	18 3 79	25	12	290	21
21	19 3 79	17	23	276	21
21	20 3 79	5	20	302	11
21	21 3 79	12	27	284	18
21	22 3 79	359	19	292	11
21	23 3 79	9	31	262	17
21	24 3 79	4	24	325	5
21	25 3 79	17	22	110	2
21	26 3 79	19	21	130	2
21	27 3 79	8	36	355	5
21	28 3 79	354	34	18	16